Available online at www.sciencedirect.com
SCIENCE DIRECT
ELSEVIER
Journal of the European Ceramic Society 26 (2006) 1411–1419
ECERS
www.elsevier.com/locate/jeurceramsoc

Microscale computational simulation and experimental measurement of thermal residual stresses in glass–alumina functionally graded materials

V. Cannillo [a,*], M. Montorsi [a], C. Siligardi [a], A. Sola [a], G. de Portu [b], L. Micele [b], G. Pezzotti [c]

[a] *Dipartimento di Ingegneria dei Materiali e dell'Ambiente, University of Modena e Reggio Emilia, Via Vignolese 905/A, 41100 Modena, Italy*
[b] *Institute of Science and Technology for Ceramics, Via Granarolo, 64-48018 Faenza, Italy*
[c] *Research Institute for Nanoscience (RIN), Ceramic Physics Laboratory, Kyoto Institute of Technology (KIT), Sakyo-ku, Matsugasaki 606, 8585 Kyoto, Japan*

Received 22 December 2004; received in revised form 21 February 2005; accepted 25 February 2005
Available online 5 April 2005

Abstract

Glass–alumina functionally graded materials are new attractive composite materials, that can achieve peculiar mechanical properties due to their gradual compositional variation. Nevertheless, the difference between the coefficients of thermal expansion of the constituent phases may result in significant thermal residual stresses in service or during fabrication. A proper glass formulation can minimize the mismatch in thermo-mechanical properties, thus relevantly reducing the mean value of the resultant thermal stresses. However, it is a crucial requirement to evaluate the effect of microstructural discreteness and randomness on the actual stress distribution in functionally graded materials. With this aim, a computational model which applies the finite element method at the microscale is used. The careful modelling of the real microstructural details enables to accurately predict the local stress values and distribution. In order to verify the reliability of the computational simulations, the residual thermal stresses were also experimentally measured by means of a piezo-spectroscopic technique. The comparison between the numerical and the experimental results validate the microstructure-based model.

Keywords: Microstructure; Mechanical properties; Thermal expansion; Al_2O_3; Glass

1. Introduction

Functionally graded materials are a new class of composite materials, whose peculiarity lies in the uneven, engineered spatial distribution of the constituent phases. The controlled compositional and microstructural gradient is associated with a spatial change in properties, which can be tailored to the prescribed application.[1,2]

The idea of functionally graded materials was first explicitly developed in Japan at the end of the 1980s, in the context of a research project for the relaxation of thermal stresses.[3] Initially, high performance thermal barrier coatings for aerospace applications were developed. Such thermal coatings coupled a metallic phase, which provided mechanical toughness and thermal conductivity on one side, and a ceramic phase, which ensured thermal resistance and insulation on the other side. However, if the two heterogeneous materials were directly bonded, this could result in high thermal residual stresses due to the mismatch in thermo-mechanical properties. Yet the thermal stresses could be significantly reduced by means of a gradual change in system composition and microstructure.[4]

In order to tailor a functionally graded material to a prescribed thermo-mechanical loading, it would be desirable to correlate its properties and microstructure. The continuous approach, which assumes that the FGM microstructure and related properties vary continuously and smoothly in space, has been widely used in the past, because of its relative simplicity. Such continuous model, however, can be reasonably applied only if the dimensional scale considered is much larger than the mean grain size of the constituent phases.[5]

* Corresponding author. Tel.: +39 059 2056240; fax: +39 059 2056243.
E-mail address: valeria@unimo.it (V. Cannillo).

0955-2219/$ – see front matter © 2005 Elsevier Ltd. All rights reserved.
doi:10.1016/j.jeurceramsoc.2005.02.012

As a matter of fact, the FGM microstructure is intrinsically discrete and stochastic, since it is possible to identify distinct domains of finite dimensions made up of different ingredient materials.[6,7] The microstructural heterogeneities are likely to induce local stress concentrations which, in turn, may lead to local damages and finally large-scale failures. A reliable predictive model, therefore, should take into consideration the real FGM microstructural morphology.

This work aims at evaluating the effect of discreteness and randomness of the real FGM microstructure on the thermal residual stress distribution. In particular, the analysis is focused on a glass–alumina functionally graded material. Since thermal residual stresses are likely to cause cracks in brittle materials, the ingredient materials were carefully chosen, thus minimizing the mismatch in their coefficients of thermal expansion. Then, in order to check the actual stresses caused by the thermal treatment, both a computational method and an experimental approach were applied.

In the past, Jitcharoen et al.[8,9] widely investigated a similar system, obtained by means of percolation of a $CaO–Al_2O_3–SiO_2$ glass into an alumina substrate. The authors computationally predicted and experimentally proved that the gradual change in elastic properties, especially the Young modulus, significantly improved the superficial properties, in terms of Hertzian cone crack resistance, of the functionally graded materials with respect to the single constituent phases or a traditional, not graded, composite material. In this study a $CaO–ZrO_2–SiO_2$ glass was utilized, since the glasses belonging to this ternary system usually exhibit interesting mechanical properties, such as a high Young modulus and a relatively good fracture toughness.[10,11] Moreover, the absence of any aluminum oxide in the composition made easier the final FGM characterization. As already mentioned, the glass formulation was designed with the intention of minimizing the mismatch in coefficients of thermal expansion between the alumina and the glass itself. This is a crucial requirement in order to reduce the thermal residual stresses which may arise at the microscale, next to the glass–alumina interface, while cooling down from the processing temperature.

The thermal residual stress values and distribution were predicted by using an image-based computational tool which maps digitalized microstructural images onto finite element meshes. The computational model, however, was experimentally validated measuring the thermal residual stresses on a FGM specimen by means of a refined piezo-spectroscopy technique, based on the chromophoric fluorescence of Cr^{3+} impurities in the Al_2O_3 substrate.

2. Materials

2.1. Ingredient materials

As already mentioned, this work focused on glass–alumina functionally graded materials. Since the experimental preparation and characterization of the ingredient materials, as well as the final FGMs, have been accurately described elsewhere,[11] they are only briefly summarized here.

Table 1
Ingredient materials properties[11,12]

Ingredient materials	Young modulus (GPa)	Poisson ratio	Coefficient of thermal expansion ($\times 10^{-6}\,^{\circ}C^{-1}$)
Glass	96	0.27	8.7
Alumina	358	0.20	8.2

Industrial, high-purity α-alumina tiles were used as substrates. The alumina, produced via sintering, was a polycrystalline system with a residual porosity of about 4.2 vol.%. As for the glass phase, a composition belonging to the $CaO–ZrO_2–SiO_2$ ternary system was chosen. The most relevant thermo-mechanical properties of the constituent phases were experimentally measured and reported in Table 1.[11,12]

A glass and an alumina samples were cut and used as standards in the thermal stress measurement.

2.2. Functionally graded materials

The FGM samples were obtained by means of percolation of the molten glass into the alumina substrate.[13] A glass slice, about 1 mm thick, was placed onto the upper face of a small alumina tile, about 25 mm × 25 mm × 8 mm, and heat treated following a properly designed heating cycle.[11]

The obtained functionally graded materials were carefully investigated. An X-ray diffraction analysis was performed in order to check the mineralogical evolution of the system. The diffraction pattern proved that neither the heat treatment nor the glass infiltration induced the crystallization of new phases.[11] The FGM cross-section was observed under a SEM–EDS and the molar concentrations of Al_2O_3 and SiO_2 (assumed as a glass marker) were measured as a function of depth. According to the chemical analysis, the glass reached a depth of about 800 μm.[11] It is worth noting, however, that the EDS curve was not strictly monotonic, since the chemical analysis was punctual in nature, while the FGM microstructure resulted to be discrete and stochastic.

In order to make the microstructural morphology more evident, a FGM cross-section was chemically etched with a 4% hydrofluoric acid (HF) for 10 s at room temperature. The selective acid corrosion removed the glass, but the alumina grains were not modified. An example of the resultant microstructure is reported in Fig. 1. While the FGM cross-section was observed under the scanning electron microscope, several partially overlapped photographs were saved in a digital format and then joined, in order to build an image of the entire graded profile. The resulting picture represented a 100 μm wide, 800 μm deep cross-section area.

Finally a functionally graded material specimen was sliced, thus obtaining a sample suitable for the experimental thermal stress measurement.

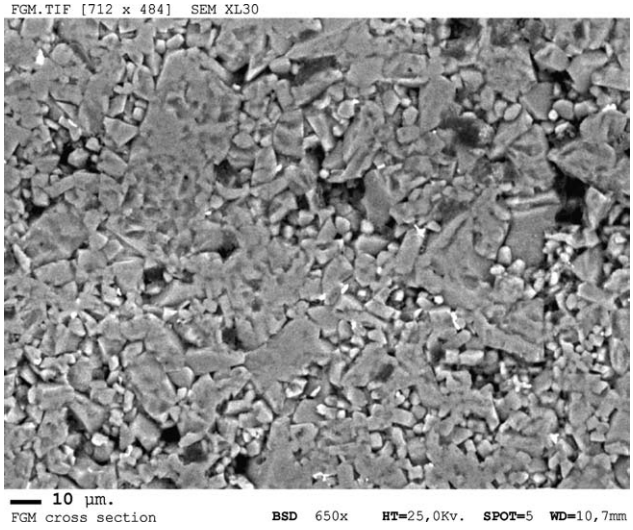

Fig. 1. BSD–SEM image showing the glass–alumina FGM microstructure (at a depth of about 100 μm) The specimen cross-section was previously chemically etched with a 4% hydrofluoric acid (HF) for 10 s at room temperature in order to make the microstructural morphology more evident.

3. Method

Thermal residual stresses in FGMs can be hardly evaluated by means of analytical approaches, due to the non-linearity of the governing equations.[14] As a consequence, the finite element method has been widely used to predict the thermal residual stress distribution in both continuously[15] and multilayered[16] functionally graded materials. The achieved numerical results may be useful to optimize the compositional gradient, reducing damages caused by residual stresses.[17–19] In order to validate the numerical analysis, various experimental techniques have been applied. X-ray diffraction, for example, is a non destructive approach which can be used to assess the surface stress condition,[20–22] while neutron diffraction[23,24] or synchrotron radiation[22] methods are required to investigate the interior of the material. As already mentioned, in the present work the theoretical results obtained via a microscale FEM simulation were compared with the experimental data acquired by means of a piezospectroscopic technique.

3.1. Modeling procedure

The computational simulations were carried out by using OOF,[25,26] a software which applies the finite element method at the microscale, by using microstructural images and materials properties as input data. The preprocessor is able to acquire microstructural images, such as digitalized scanning electron microscope (SEM) photographs, and directly create two-dimensional finite element meshes on them. The materials properties of the constituent phases are set as input data. Then OOF, the FEM solver, is able to perform virtual experiments on the grids.

Since it is a computational tool operating at the microscale, OOF has already been used in order to correlate materials properties to microstructure. In particular, this code has been widely exploited for composite materials and heterogeneous systems, as the finite element grids carefully model the microstructural details, such as the shape and dimensions of inclusions. For example, several authors investigated the distribution of residual stresses in polycrystalline and complex materials.[27–34] Moreover, phenomena related to fracture behaviour in heterogeneous and composite systems were throughly analyzed in terms of microcracking, crack propagation, damage accumulation, toughening mechanism and reliability.[35–41]

In the present work, each SEM image was acquired by the pre-processor, the constituent phases were identified and the correspondent materials properties were assigned according to Table 1. Finally the finite element mesh was created, which contained about 92,200 elements. Besides the alumina and the glass, the residual pores were taken in consideration as a third phase with no stiffness.[25] An example of the finite element mesh is presented in Fig. 2.

Since this work aimed at evaluating the thermal residual stresses which may arise during the FGM fabricating process because of the mismatch in the coefficients of thermal expansion, it was assumed that the critical step was the cooling down after the thermal treatment. In particular, below the glass transition temperature, the glass viscosity becomes so high that the stresses can not be relaxed anymore. Therefore, in the computational model, a temperature decrease ΔT of $-770\,^{\circ}\mathrm{C}$ was considered, between the glass transition temperature, which was experimentally measured to be 790 °C,[11] and room temperature. Once the temperature gradient was assigned as an input parameter, the resultant thermal residual stresses were evaluated. In the simulations performed, the plane stress hypothesis was assumed. By means of the finite

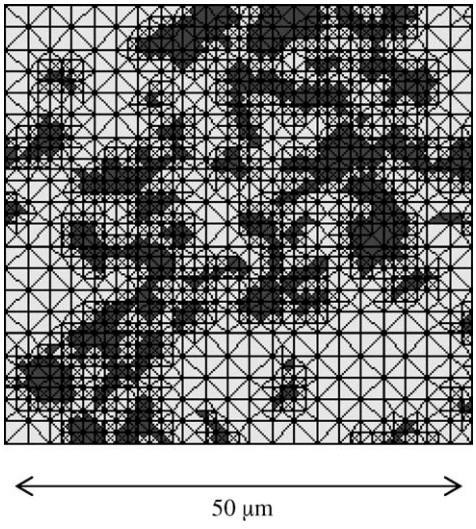

Fig. 2. Example of the finite element mesh (detail) which was created at the microscale: the SEM image was directly acquired and mapped onto a triangular elements mesh.

element solver, it was possible to create maps of the actual local stress distribution. Moreover, in order to estimate the mean value of the thermal stresses, the mean stress of the alumina and the glass was calculated for 8 equal regions of the profile image, each of which represented a 100 μm wide and 100 μm deep area. In order to validate the reliability of the computational model, the residual thermal stresses were experimentally quantified.

3.2. Experimental measurement

The stress field distribution along the cross-section of infiltrated samples was determined by using piezo-spectroscopy techniques related to the characteristic R1, R2 doublet produced by chromophoric fluorescence of Cr^{3+} impurities in Al_2O_3. The principle of relating an observed line shift in a fluorescence spectrum to the state of stress has been described previously by Grabner.[42] When polycrystalline Al_2O_3 (having a fine grained microstructure and no significant texture) is subjected to a stress σ, the change in frequency $\Delta\nu$ in luminescence line is given by the tensorial relationship

$$\Delta\nu = \frac{1}{3}\Pi_{ii}\sigma_{jj} \quad (1)$$

where Π_{ii} is referred to as the piezo-spectroscopic coefficient (i.e., relating frequency to stress).

The spectrometer apparatus (ISA, T 64000 Jovin-Yvon) employed in the present experiments used, as excitation source, an argon-ion laser operating at a wavelength of 488 nm with a power of 200 mW. For obtaining micron-scale magnification, an optical microscope lens was used both to focus the laser on the sample and to collect the scattered signal. Scattered frequencies were analyzed with a triple monochromator equipped with a charge coupled device (CCD) camera. When focussed by an optical microscope, the dimension of the laser spot on the samples was 1 μm (i.e., using a ×100 optical lens). Thermal and instrumental fluctuations were compensated by monitoring the spectrum from a Hg/Ne discharge lamp. The recorded spectra were analysed with a commercial software (LabSpec 4.02, Horiba/Jobin-Ivon). The frequency shifts were obtained by subtracting from the centre of the peak recorded under stress the centre of the peak in the unstressed state. The frequency used as a standard value for zero external stress was obtained from the porous Al_2O_3 aged 4 h at 1600 °C without glass, acquiring an array of 100 spectra on the surface and averaging all the values of the peak centre.

An important characteristic of the piezo-spectroscopic techniques is that the average uniaxial piezo-spectroscopic coefficient, Π_{uni}, characterizing the linear dependence of the peak shift on stress, strongly depends on many parameters specific of the material, especially in processing derived parameters such as grain size, presence of other phases, porosity, etc. Hence, a preliminar calibration procedure is required case by case for determining the Π_{uni} value pertinent to each material. For this purpose, bending bars were mounted on a four-point bending jig under the optical microscope and loaded with a known load below fracture stress; after the load was applied, the whole jig was moved under the microscope and spectra recorded every 150 μm from the compressive towards the tensile side of the specimen. The load was then converted to stress, σ, using the standard four-point-bending elastic equation and the peak shift, $\Delta\nu$, plotted as a function of the applied stress. The average Π_{uni} was obtained from the slope of the σ versus $\Delta\nu$ plot.

Microscopic stress distributions were measured by collecting linear profiles of spectra on the specimen cross-sections. The automatically collected profiles of spectra were 5 μm-spaced. Specimens were placed on a mapping device (lateral resolution of 0.1 μm), which was connected to a personal computer to drive highly precise displacements (along both *X* and *Y* axes) on the specimen surface.

4. Results

4.1. Computational simulations

The stress distribution could be visualized via maps, which are presented in Fig. 3. As expected, since the glass

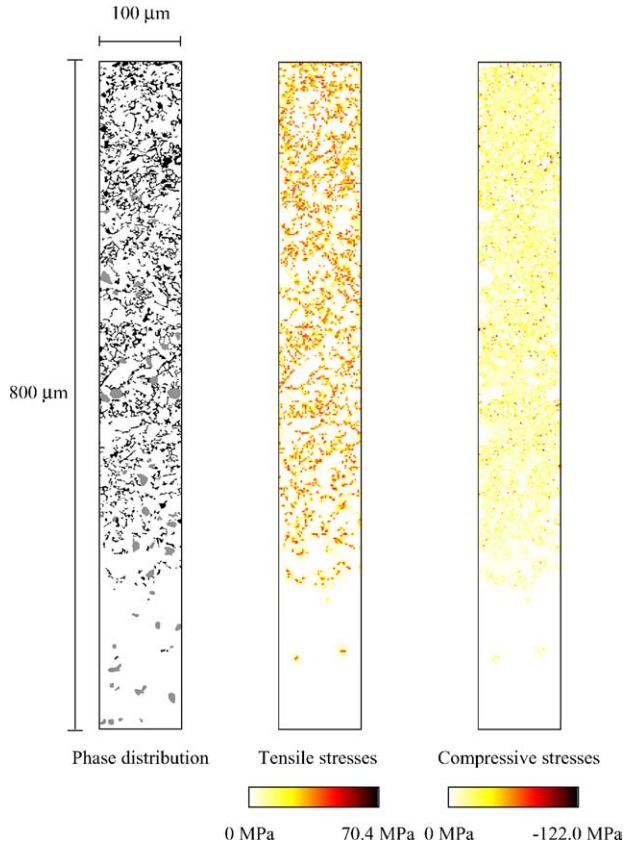

Fig. 3. The tensile and compressive thermal residual stresses were calculated in the cross-section image; in the picture representing the phase distribution, the white areas stand for alumina, the black ones for glass and the gray ones for pores.

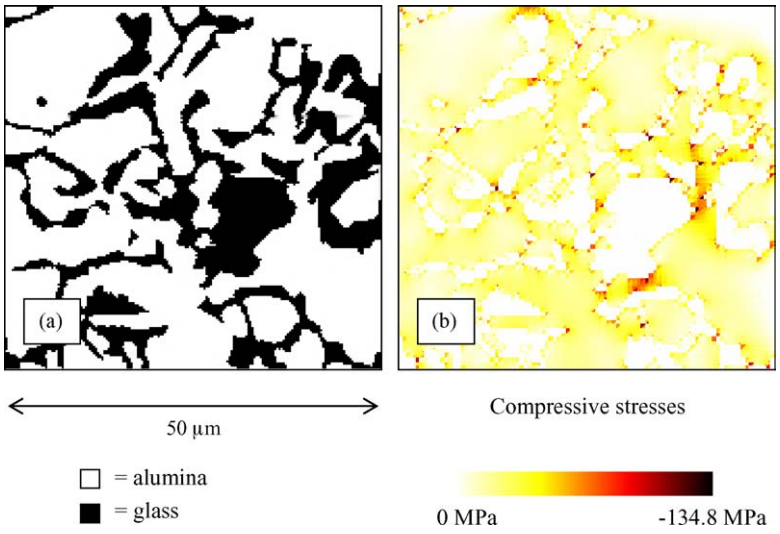

Fig. 4. Comparison between (a) the distribution of the ingredient materials; and (b) the distribution of compressive residual stresses. The compressive residual stresses are mainly located in the alumina; on average, they are low in value but some peak stresses arise at the glass–alumina interface, especially when a thin strip of alumina separates two glass domains.

coefficient of thermal expansion is higher than the alumina one, the thermal residual stresses are mainly tensile in the glass and mainly compressive in the alumina. On average, the stresses are low in value; some peak stresses, however, can be detected at the glass–alumina interface, as illustrated in Fig. 4.

In each of the eight considered areas, in which the profile image was subdivided, the average values of the principal stresses were evaluated both in the glass and the alumina; then the mean hydrostatic stress was calculated for each phase, i.e.,

$$\bar{\sigma} = \frac{\sigma_{\mathrm{I}} + \sigma_{\mathrm{II}} + \sigma_{\mathrm{III}}}{3} \tag{2}$$

The mean hydrostatic stress, which is representative of the stress tensor, is depicted in Fig. 5 as a function of depth. In particular, graphs "a" and "b" refer to the alumina and the glass phase, respectively. Such stresses are very low in value in both the ingredient materials, glass and alumina.

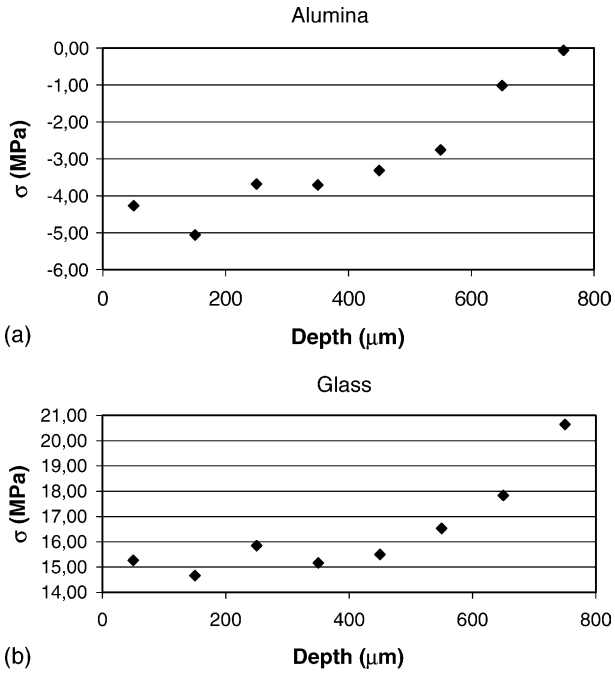

Fig. 5. The mean hydrostatic stress as a function of depth. In particular, graphs (a) and (b) refer to the alumina and the glass phase, respectively.

4.2. Experimental

Fig. 6 shows the stress dependence of the R1 band from −110 to +120 MPa. The slope of the linear least square was assumed to be the uniaxial piezo-spectroscopic coefficient (the value relating frequency to stress). Whereas, sapphire has a different coefficient Π_{ii} for each crystallographic axis,[43] the Al_2O_3 prepared according Section 2 is supposed to be polycrystalline and without any significant texture, so that the uniaxial coefficient is one of the three identical elements of the diagonal of piezo-spectroscopic tensor Π_{ii}. To calculate the mean hydrostatic stress, the following simplification was done

$$\bar{\sigma} = \frac{\sigma_{\mathrm{I}} + \sigma_{\mathrm{II}} + \sigma_{\mathrm{III}}}{3} = \frac{\Delta\nu/\Pi_{11} + \Delta\nu/\Pi_{22} + \Delta\nu/\Pi_{33}}{3} = \frac{1}{3}\Delta\nu\left(\frac{1}{\Pi_{\mathrm{uni}}} + \frac{1}{\Pi_{\mathrm{uni}}} + \frac{1}{\Pi_{\mathrm{uni}}}\right) = \frac{1}{3}\Delta\nu\left(\frac{3}{\Pi_{\mathrm{uni}}}\right) = \frac{\Delta\nu}{\Pi_{\mathrm{uni}}} \tag{3}$$

where $\Delta\nu$ is the shift of R1 peak.

Table 2 summarizes the salient piezo-spectroscopic characteristics of the Al_2O_3 studied in the present investigation; the R1 and R2 values are based on the alumina fluorescence spectrum. The peak used in stress measurement was R1, because of its higher correlation coefficient and the consequent

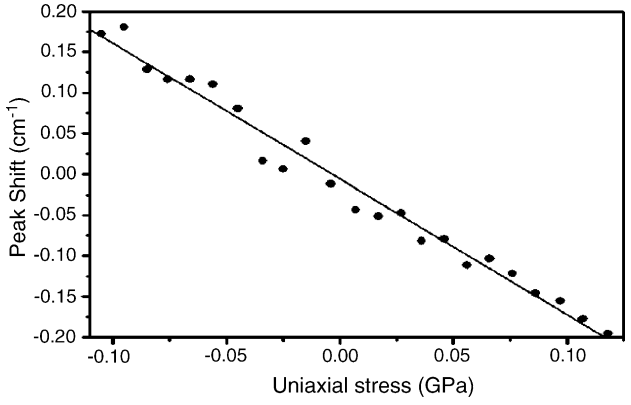

Fig. 6. Stress dependence of the position of R1 band.

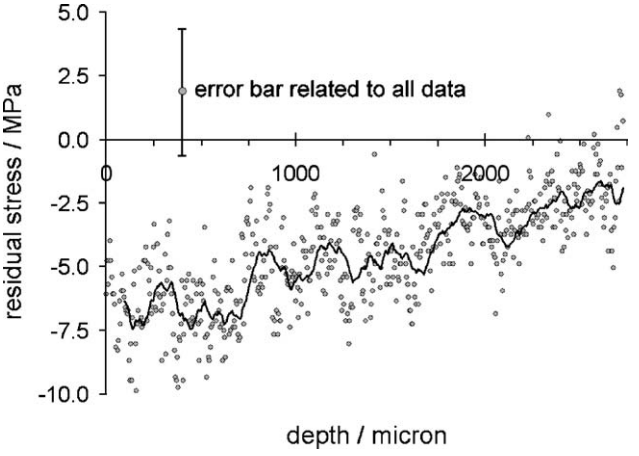

Fig. 7. Measured stress field distribution in the cross-section of infiltrated specimen. For more clearness, error bar (±2.5 MPa) is showed only in the caption.

lower scattering of data. The value of Π_{hydro} (= 3 Π_{uni}) is significantly lower than the value measured by previous authors for other types of Al_2O_3 (sapphire,[43] polycrystalline[42,44]): the reason of the rather large deviation of R1 stress dependence may reside in the porosity of the material, that can affect both mechanical and spectroscopic (i.e., with a high light scattering) properties.

The graph of Fig. 7 shows the residual stress profile along the cross-section. Given that the piezo-spectroscopic technique is related to Al_2O_3 fluorescence spectrum, the stress value measured refers solely to the Al_2O_3 phase; actually, no stress assessment on the glass phase by piezo-spectroscopy was possible. Furthermore, data appear noisy for the reason that the stress value is close to the sensitivity of the piezo-spectroscopic technique: it should be considered a confidence interval of ±2.5 MPa. In the area containing glass, Al_2O_3 phase undergoes a weak compressive stress. A fairly regular decrease of the stress from −8 MPa to a negligible value corresponding to the progressive decrease of the glass content can be seen from the surface to a depth of about 2750 μm.

5. Discussion

Several applications of optimized functionally graded materials benefit from the reduction of thermal residual stresses which may be reached when an abrupt bi-material junction is replaced by a gradual change in composition and/or microstructure. On the other hand, the microstructure of functionally graded materials is typically discrete and stochastic, since at the microscale it is possible to identify distinct domains having different compositions and therefore dissimilar thermo-mechanical properties. As a consequence, a microscale model is required in order to have a realistic view of the thermal residual stresses which may locally arise between the constituent phases. In the past, Dao et al.[45] proposed a micromechanical study of thermal residual stresses in functionally graded materials. By applying the finite element method to a discrete micromechanics model, they demonstrated that the existence of adjacent grains, randomly distributed and made up of heterogeneous phases, could result in locally concentrated thermal residual stresses. This micromechanics model, however, assimilated each grain to a square domain, thus neglecting the actual microstructural details.

The micromechanical approach applied in this work provides for an accurate modelling of the real microstructural details, which may be responsible for local stress concentrations. As a matter of fact, the simulations performed on the full-profile image suggest that the thermal residual stresses, that are mainly tensile in the glass and compressive in the alumina, are on average quite low in value. This result is consistent with the aforementioned values of the coefficients of thermal expansion, which are really similar, the glass one being slightly greater than the alumina one. Actually it is worth noting that the optimization of the glass composition, by minimizing the mismatch in thermo-mechanical properties, allows to keep the mean thermal residual stresses really low in value. Yet, the maps describing the actual stress distribution show that some peak stresses can be locally generated at the glass–alumina interface, especially when a thin strip of alumina separates two glass domains, as shown in Fig. 4.

As far as the numerically determined mean hydrostatic stress is concerned (Fig. 5), though its value was averaged

Table 2
Salient piezo-spectroscopic characteristics of the investigated Al_2O_3.

Peak	Π_{uni} ($cm^{-1}\,GPa^{-1}$)	Π_{hydro} ($cm^{-1}\,GPa^{-1}$)	R^2	Unstressed value (cm^{-1})	Unstressed value (nm)
R1	-1.6_7	−5.0	0.98	14407.55	694.080
R2	-1.8_6	−5.4	0.96	14437.67	692.633

on each of the eight areas, the graphs make clear that the trend is not strictly monotonic. Qualitatively, however, at increasing depths the mean hydrostatic stress value becomes higher in the glass (from 14.66 to 20.64 MPa), while it becomes lower (in modulus) in the alumina (from −5.06 MPa to −0.06 MPa). It is likely that the residual thermal stress variation as a function of depth is related to the compositional gradient. As a matter of fact, when increasing depths are considered, the glass volume fraction decreases, while the alumina volume fraction increases. Similarly the fluctuations of the predicted thermal residual stresses may be due to stochastic microscale deviations of the real constituent phase distribution with respect to the macroscale compositional gradient. Moreover, the SEM micrographs show that the glass zones are larger and more irregular in the upper profile regions than in the lower ones and the size and shape of the glass domains may affect the thermal residual stresses. In a previous work, V. Cannillo et al.[33] proposed a numerical model for the prediction of thermal residual stresses in alumina–glass composite materials. The computational tests demonstrated that the thermal stresses depend not only on the reinforcement volume fraction, but also on the particle shape. These results do not apply quantitatively to the functionally graded materials analyzed here, since they refer to a different system, a traditional, not graded composite material, with alumina platelets uniformly dispersed in a glass matrix. However, they confirm that the microstructural morphology, as well as the composition, influences the thermal residual stresses.

Finally, a really important target of this work was to check the reliability of the micromechanical model. In this intent, the thermal residual stresses in the alumina phase were experimentally quantified by means of piezo-spectroscopy techniques and the results were compared with the numerical prediction of the hydrostatic stress. The measured curves show that, moving from the free surface to the maximum depth reached by the glass, the alumina stress values progressively decrease in modulus, though the trend is not perfectly monotonic (Fig. 7). However, it should be noted that the compressive stresses in the alumina decrease up to zero at a depth of 800 μm in the computational model, whilst in the experimental determination such depth is 2750 μm. This discrepancy can be attributed to the fact that the computational model relies on SEM acquired micrographs and EDS analysis. With EDS measurements, however, weight concentrations below 1% can not be detected.[46] Since the SiO_2 content has been assumed as the glass marker, and since the SiO_2 amount in the glass is about 50%, it follows that this technique is not able to reveal the presence of glass below 2%. It is likely that between 800 and 2750 μm the glass content is below the EDS detectability threshold. This could explain the difference in the profiles computationally and experimentally determined, keeping in mind that a 2% glass content would cause a weak compressive stress in the alumina. Moreover, it should be pointed out that the experimentally measured stress value is close to the sensitivity of the piezo-spectroscopic technique and that a confidence interval of ±2.5 MPa appears to be realistic. Therefore, the discrepancy which may be noticed between the predicted and the measured values is within the error bar. It can be concluded that the experimental data and the computational simulations are qualitatively in fairly good agreement.

Thus, the acceptable agreement between experimental measurements and numerical predictions confirms the reliability of the micromechanical model. It is worth noting, however, that while the piezospectroscopic technique is able to measure only the mean value of the residual stresses in the alumina, the microscale computational approach provides the actual stress distribution in both the ingredient materials. However, the experimental technique is essential to validate the model.

6. Conclusions

This work focused on the thermal residual stresses which may be caused in functionally graded materials by the mismatch in the coefficients of thermal expansion of the ingredient materials. Indeed, due to the microstructural discreteness and randomness of FGMs, distinct domains of heterogeneous composition may be identified at the microscale and residual thermal stresses may arise at the interfaces. Moreover, even if the mean value of the thermal residual stresses is low, local stress concentrations are likely to be generated. Such stress concentrations in brittle materials are critical, since they may cause a local crack initiation. As a consequence, a reliable computational model should account for the real FGM microstructural morphology.

As a matter of fact, the microscale simulations proved that the minimization of the mismatch in thermo-mechanical properties of the glass and the alumina leads to really low mean values of the thermal residual stresses. However, some peak stresses arise at the interface between the ingredient materials, especially when a thin strip of one phase lies between two domains of a second phase.

In order to test the reliability of the numerical model, the residual stresses were also experimentally quantified by means of a piezo-spectroscopic technique. When compared, the predicted stresses resulted to be consistent with the experimental data, thus confirming the effectiveness of the microscale simulations, since the stresses in the alumina are compressive and low in magnitude and they decrease along the penetration direction.

Since the residual stresses turned out to be really low in value, it may be concluded that the functionally graded material was successfully designed and optimized. The selection of proper ingredient materials and the application of adequate fabrication techniques are key factors in order to obtain an engineered FGM. Besides developing a reliable FGM production method, the present research proved the effectiveness of the methodology for residual thermal stresses prediction.

Acknowledgements

Prof. W.C. Carter and OOF-NIST team[25] are gratefully acknowledged.

References

1. Miyamoto, Y., Kaysser, W. A., Rabin, B. H., Kawasaki, A. and Ford, R. G., *Functionally Graded Materials. Design, Processing and Applications*. Kluwer Academic Publishers, 1999.
2. Mortensen, A. and Suresh, S., Functionally graded metals and metal–ceramic composites. I. Processing. *Int. Mater. Rev.*, 1995, **40**(6), 239–265.
3. Rabin, B. H. and Shiota, I., Functionally gradient materials. *MRS Bull.*, 1995, **XX**(1), 14–15.
4. Koizumi, M. and Niino, M., Overview of FGM research in Japan. *MRS Bull.*, 1995, **XX**(1), 19–21.
5. Mortensen, A. and Suresh, S., Functionally graded metals and metal-ceramic composites. II. Thermomechanical behaviour. *Int. Mater. Rev.*, 1997, **42**(3), 85–116.
6. Cannillo, V., Manfredini, T., Corradi, A. and Carter, W. C., Numerical models of the effect of heterogeneity on the behavior of graded materials. *Key Engineering Materials*, *206–213*. Trans Tech Publications, Switzerland, 2002, pp. 2163–2166.
7. Cannillo, V. and Carter, W. C., Numerical models of the effect of elastic heterogeneity on the toughness of graded materials. In *Advances in Fracture Research, Proceedings of ICF10*, ed. K. Ravi-Chandar, B. L. Karihaloo, T. Kishi, R. O. Ritchie, K. Wada, A. T Yokobori Jr. and T. Yokobori, 2001.
8. Jitcharoen, J., Padture, N. P., Giannakopoulos, A. E. and Suresh, S., Hertzian-Crack suppression in ceramics with elastic-modulus-graded surfaces. *J. Am. Ceram. Soc.*, 1998, **81**(9), 2301–2308.
9. Suresh, S., Olsson, M., Giannakopoulos, A. E., Padture, N. P. and Jitcharoen, J., Engineering the resistance to sliding-contact damage through controlled gradients in elastic properties at contact surfaces. *Acta Mater.*, 1999, **47**(14), 3915–3926.
10. Leonelli, C. and Siligardi, C., $CaO\text{-}SiO_2\text{-}ZrO_2$ glasses: modelling and experimental approach. *Recent Res. Dev. Mater. Sci.*, 2002, **3**, 599–618.
11. Cannillo, V., Manfredini, T., Montorsi, M., Siligardi, C. and Sola, A., Glass–alumina functionally graded materials preparation and compositional profile evaluation, submitted for publication.
12. Cannillo, V., Manfredini, T., Montorsi, M., Siligardi, C. and Sola, A., Computational simulations for the optimisation of the mechanical properties of alumina–glass functionally graded materials. In *Computational Modeling and Simulation of Materials—Part A, in Advances in Science and Technology*, *42*, ed. P. Vincenzini and A. Lami. Techna Group s.r.l, 2004, pp. 679–686.
13. Flaitz, P. L. and Pask, J. A., Penetration of polycristalline alumina by glass at high temperatures. *J. Am. Ceram. Soc.*, 1987, **70**(7), 449–455.
14. Tanigawa, Y., Matsumoto, M. and Akai, T., Optimization of material composition to minimize thermal stresses in nonhomogeneous plate subjected to unsteady heat supply. *JSME Int. J. Ser. A: Mech. Mater. Eng.*, 1997, **40**(1), 84–93.
15. Yang, Z. M., Zhou, Z. G. and Zhang, L. M., Characteristics of residual stress in Mo–Ti functionally graded material with a continuous change of composition. *Mater. Sci. Eng. A*, 2003, **A358**(1–2), 214–218.
16. Jin, G. and Awaji, H., Residual thermal stresses in multilayered functionally graded material plates. *Mater. Sci. Res. Int.*, 2003, **9**(2), 125–130.
17. Zhang, K. P., Shen, Q., Fang, Q. and Wang, Z., Design and optimization of Al_2TiO_5/Al_2O_3 system functionally graded materials. *Key Eng. Mater.*, 2003, **249**(Composite Materials III), 141–144.
18. Huang, C., Chen, S. and Duan, Z., FEM simulations and optimization about residual stresses in coating structures with functionally graded materials layer. *Mater. Sci. Forum*, 2003, **423–425**(Functionally Graded Materials VII), 659–664.
19. Grujicic, M. and Zhao, H., Optimization of 316 stainless steel/alumina functionally graded material for reduction of damage induced by thermal residual stresses. *Mater. Sci. Eng. A*, 1998, **A252**(1), 117–132.
20. Widjaja, S., Limarga, A. M. and Yip, T. H., Modeling of residual stresses in a plasma-sprayed zirconia/alumina functionally graded-thermal barrier coating. *Thin Solid Films*, 2003, **434**(1–2), 216–227.
21. Qin, S., Jiang, D., Zhang, J. and Qin, J., Design, fabrication and properties of layered SiC/TiC ceramic with graded thermal residual stress. *J. Eur. Ceram. Soc.*, 2003, **23**(9), 1491–1497.
22. Dantz, D., Genzel, Ch., Reimers, W. and Buslaps, T., Investigations of the residual stress state in microwave sintered functionally graded materials. *Ceram. Trans.*, 2001, **114**(Functionally Graded Materials 2000), 563–570.
23. Schreiber, J., Neubrand, A., Wieder, T., Stalder, M. and Shamsutdinov, N., Distribution of macro- and micro-stresses in W-Cu FGM. *Ceram. Trans.*, 2001, **114**(Functionally Graded Materials 2000), 603–610.
24. Kesler, O., Matejicek, J., Sampath, S. and Suresh, S., Measurement of residual stress in plasma-sprayed composite coatings with graded and uniform compositions. *Mater. Sci. Forum*, 1999(Functionally Graded Materials 1998), 308–311.
25. Carter W.C., Langer S.A. and Fuller E.R., The OOF manual, version 1.0, 1998.
26. Langer, S. A., Fuller Jr., E. R. and Carter, W. C., OOF: an image-based finite-element analysis of material microstructures. *Comput. Sci. Eng.*, 2001, **3**(3), 15–23.
27. Hsueh, C. H., Fuller Jr., E. R., Langer, S. A. and Carter, W. C., Analytical and numerical analyses for two-dimensional stress transfer. *Mater. Sci. Eng. A*, 1999, **268**(1–2), 1–7.
28. Hsueh, C. H., Haynes, J. A., Lance, M. J., Becher, P. F., Ferber, M. K., Fuller Jr., E. R. *et al.*, Effects of interface roughness on residual stresses in thermal barrier coatings. *J. Am. Ceram. Soc.*, 1999, **82**(4), 1073–1075.
29. Hsueh, C. H. and Fuller Jr., E. R., Residual stresses in thermal barrier coating: effects of interface asperity curvature/height and oxide thickness. *Mater. Sci. Eng. A*, 2000, **283**(1–2), 46–55.
30. Zimmermann, A., Fuller Jr., E. R. and Rödel, J., Residual stress distributions in ceramics. *J. Am. Ceram. Soc.*, 1999, **82**(11), 3155–3160.
31. Vedula, V. R., Glass, S. J., Saylor, D. M., Rohrer, G. S., Carter, W. C., Langer, S. A. *et al.*, Residual-stress predictions in polycrystalline alumina. *J. Am. Ceram. Soc.*, 2001, **84**(12), 2947–2954.
32. Saigal, A. and Fuller Jr., E. R., Analysis of stresses in aluminum–silicon alloys. *Comput. Mater. Sci.*, 2001, **21**(1), 149–158.
33. Cannillo, V., Leonelli, C. and Boccaccini, A. R., Numerical models for thermal residual stresses in Al_2O_3 platelets/borosilicate glass matrix composites. *Mater. Sci. Eng., A*, 2002, **323**, 246–250.
34. Cannillo, V., Manfredini, T., Montorsi, M. and Boccaccini, A. R., Investigation of the mechanical properties of Mo-reinforced glass–matrix composites. *J. Non-Cryst. Solids*, 2004, **344**, 88–93.
35. Zimmermann, A., Carter, W. C. and Fuller Jr., E. R., Damage evolution during microcracking of brittle solids. *Acta Mater.*, 2001, **49**(1), 127–137.
36. Zimmermann, M. H., Baskin, D. M., Faber, K. T., Fuller Jr., E. R., Allen, A. J. and Keane, D. T., Fracture of a textured anisotropic ceramic. *Acta Mater.*, 2001, **49**(16), 3231–3242.
37. Saigal, A., Fuller Jr., E. R., Langer, S. A., Carter, W. C., Zimmerman, M. H. and Faber, K. T., Effect of interface properties on microcracking of iron titanate. *Scr. Mater.*, 1998, **38**(9), 1449–1453.
38. Cannillo, V. and Carter, W. C., Computation and simulation of reliability parameters and their variations in heterogeneous materials. *Acta Mater.*, 2000, **48**(13), 3593–3605.
39. Cannillo, V., Leonelli, C., Manfredini, T., Montorsi, M. and Boccaccini, A. R., Computational simulations for the assessment of the

mechanical properties of glass with controlled porosity. *J. Porous Mater.*, 2003, **10**(3), 189–200.
40. Cannillo, V., Corradi, A., Leonelli, C. and Boccaccini, A. R., A simple approach for determining the in situ fracture toughness of ceramic platelets used in composite materials by numerical simulations. *J. Mater. Sci. Lett.*, 2001, **20**, 1889–1891.
41. Cannillo, V., Pellacani, G. C., Leonelli, C. and Boccaccini, A. R., Numerical modeling of the fracture behavior of a glass matrix composite reinforced with alumina platelets. *Compos. Part A*, 2003, **34**, 43–51.
42. Grabner, L., Spectroscopic technique for the measurement of residual stress in sintered Al_2O_3. *J. Appl. Phys.*, 1978, **49**, 580–583.
43. He, J. and Clarke, D. R., Determination of the piezospectroscopic coefficients for chromium-doped sapphire. *J. Am. Ceram. Soc.*, 1995, **78**(5), 1347–1353.
44. De Portu, G., Micele, L., Pezzotti, G. and Sekiguchi, Y., Measurement of residual stress distributions in Al_2O_3/3Y-TZP multilayered composites by fluorescence and Raman microprobe piezo-spectroscopy. *Acta Mater.*, 2005, **53**(5), 1511–1520.
45. Dao, M., Gu, P., Maewal, A. and Asaro, R. J., A micromechanical study of residual stresses in functionally graded materials. *Acta Mater.*, 1997, **45**(8), 3265–3276.
46. Goldstein, J. I. *et al.*, *Scanning Electron Microscopy and X-ray Microanalysis* (*2nd ed.*). Plenum Press, New York, London, 1994.